



The University of Oklahoma

arXiv: [hep-ph]  
OU-HEP-150508  
CYCU-HEP-15-04  
September 2015

## Flavor Changing Heavy Higgs Interactions at the LHC

Baris Altunkaynak<sup>a\*</sup>, Wei-Shu Hou<sup>b†</sup>, Chung Kao<sup>a‡</sup>, Masaya Kohda<sup>c§</sup>, Brent McCoy<sup>a¶</sup>

<sup>a</sup>*Homer L. Dodge Department of Physics and Astronomy,  
University of Oklahoma, Norman, OK 73019, USA*

<sup>b</sup>*Department of Physics, National Taiwan University, Taipei 10617, Taiwan, ROC*

<sup>c</sup>*Department of Physics, Chung-Yuan Christian University, Chung-Li 32023, Taiwan, ROC*

(Dated: October 13, 2015)

### Abstract

A general two Higgs doublet model (2HDM) is adopted to study the signature of flavor changing neutral Higgs (FCNH) decay  $\phi^0 \rightarrow t\bar{c} + \bar{t}c$ , where  $\phi^0$  could be a CP-even scalar ( $H^0$ ) or a CP-odd pseudoscalar ( $A^0$ ). Measurement of the light 125 GeV neutral Higgs boson ( $h^0$ ) couplings at the Large Hadron Collider (LHC) favor the decoupling limit or the alignment limit of a 2HDM, in which gauge boson and diagonal fermion couplings of  $h^0$  approach Standard Model values. In such limit, FCNH couplings of  $h^0$  are naturally suppressed by a small mixing parameter  $\cos(\beta - \alpha)$ , while the off-diagonal couplings of heavier neutral scalars  $\phi^0$  are sustained by  $\sin(\beta - \alpha) \sim 1$ . We study physics background from dominant processes with realistic acceptance cuts and tagging efficiencies. Promising results are found for the LHC running at 13 or 14 TeV collision energies.

PACS numbers: 12.60.Fr, 12.15Mm, 14.80.Ec, 14.65.Ha

---

\* E-mail address: baris@physics.ou.edu

† E-mail address: wshou@phys.ntu.edu.tw

‡ E-mail address: kao@physics.ou.edu

§ E-mail address: mkohda@cycu.edu.tw

¶ E-mail address: mccoy@physics.ou.edu

## I. INTRODUCTION

The Standard Model (SM) is very successful in explaining almost all experimental data to date, culminating in the recent discovery of the long awaited Higgs boson at the CERN Large Hadron Collider (LHC) [1, 2]. In the SM, all elementary particles acquire mass from a single Higgs doublet that generates spontaneous electroweak symmetry breaking (EWSB). All charged fermions have their masses and Yukawa couplings to the Higgs boson as correlated but free parameters. Furthermore, there are no flavor changing neutral currents (FCNC) mediated by gauge interactions, nor by Higgs interactions (FCNH), at the tree level. The most important goals of the LHC, at Run 2 and beyond, are the study of Higgs properties and the search for signals, direct or indirect, of new physics beyond the SM.

As the most massive particle ever discovered, the top quark might provide clues to better understand the mechanism of EWSB. A possible explanation for its heaviness could be provided by a special two Higgs doublet model for the top quark (T2HDM) [3], where it is the only fermion that couples to a Higgs doublet with a large vacuum expectation value (VEV). The second heaviest particle is the newly discovered Higgs boson ( $h^0$ ). With  $m_{h^0} < m_t$ , it opens up the possibility of top quark decays into  $h^0$  plus a charm quark. The branching fraction of  $t \rightarrow ch^0$  in SM at one loop level is approximately  $3 \times 10^{-15}$  [4–6] for  $m_{h^0} \simeq 120$  GeV. If this decay is detected, it would indicate a large effective FCNH coupling of tree-level origins [7], or very large enhancement from beyond SM loop effects [6].

In flavor conserving two Higgs doublet models, a discrete symmetry [8–10] is often imposed to distinguish the SU(2) doublet fields  $\phi_1$  from  $\phi_2$ . Without such a discrete symmetry, a general two Higgs doublet model (2HDM) should possess FCNH vertices. To study such interactions, we adopt the following Lagrangian involving Higgs bosons and fermions [11, 12],

$$\begin{aligned} \mathcal{L}_Y = & \frac{-1}{\sqrt{2}} \sum_{F=U,D,L} \bar{F} \{ [\kappa^F s_{\beta-\alpha} + \rho^F c_{\beta-\alpha}] h^0 + [\kappa^F c_{\beta-\alpha} - \rho^F s_{\beta-\alpha}] H^0 - i \operatorname{sgn}(Q_F) \rho^F A^0 \} P_R F \\ & - \bar{U} [V \rho^D P_R - \rho^{U\dagger} V P_L] D H^+ - \bar{\nu} [\rho^L P_R] L H^+ + \text{H.c.}, \end{aligned} \quad (1)$$

where  $P_{L,R} \equiv (1 \mp \gamma_5)/2$ ,  $c_{\beta-\alpha} = \cos(\beta - \alpha)$ ,  $s_{\beta-\alpha} = \sin(\beta - \alpha)$ ,  $\tan \beta \equiv v_2/v_1$ , and  $\alpha$  is the mixing angle between neutral Higgs scalars in the Type II (2HDM-II) notation [9].  $\kappa$  matrices are diagonal and fixed by fermion masses to  $\kappa^F = \sqrt{2} m_F / v$  with  $v \simeq 246$  GeV, while  $\rho$  matrices are free and have both diagonal and off-diagonal elements. We adopt a CP conserving Higgs model and choose  $\rho$  matrices to be real but not necessarily Hermitian.  $U$ ,  $D$ ,  $L$  and  $\nu$  are vectors in flavor space ( $U = (u, c, t)$ , etc.).  $h^0$  and  $H^0$  are CP-even scalars ( $m_h \leq m_H$ ), while  $A^0$  is a CP-odd pseudoscalar.

With the advent of the LHC, theoretical interest in search of FCNH top decays ( $t \rightarrow ch^0$ ) picked up [13–16], and the ATLAS and CMS experiments have already placed the branching fraction limit  $\mathcal{B}(t \rightarrow ch^0) < 5.6 \times 10^{-3}$  [17], implying  $\sqrt{\lambda_{htc}^2 + \lambda_{hct}^2} < 0.14$ . For LHC at  $\sqrt{s} = 14$  TeV and integrated luminosity of  $L = 3000 \text{ fb}^{-1}$ , the ATLAS experiment expects [18] to reach  $\mathcal{B}(t \rightarrow ch^0) < 1.5 \times 10^{-4}$ , i.e. probing down to  $\lambda_{htc} = \rho_{tc} \cos(\beta - \alpha) / \sqrt{2} < 0.024$ .

The flavor changing heavy Higgs decay ( $H^0 \rightarrow t\bar{c} + \bar{t}c$ ) is complementary to FCNH top decay ( $t \rightarrow ch^0$ ), since the coupling  $\lambda_{htc}$  is proportional to  $\cos(\beta - \alpha)$  while  $\lambda_{Htc} \propto \sin(\beta - \alpha)$ . Higgs boson data from the LHC favor the decoupling limit [19] or the alignment limit [20, 21] of a 2HDM. In this limit, FCNH couplings of  $h^0$  are naturally suppressed by small  $\cos(\beta - \alpha)$ , while off-diagonal couplings of  $H^0$ ,  $A^0$  are sustained by  $\sin(\beta - \alpha) \sim 1$ .

In this letter, we study the discovery potential of the LHC in the search for heavy Higgs bosons  $H^0$  or  $A^0$  that decay into a top quark and a charm quark. The top quark then

decays into a  $b$  quark, a charged lepton ( $e$  or  $\mu$ ), and a neutrino. Taking LHC Higgs data and  $B$  physics constraints into account, we evaluate production rates with full tree-level matrix elements for both signal and background. We optimize the acceptance cuts to effectively reduce the latter with realistic  $b$ -tagging and mistag efficiencies. Promising results are presented for the LHC with  $\sqrt{s} = 13$  TeV as well as 14 TeV.

## II. CONSTRAINTS FROM DATA

In this section, we apply the latest results from LHC Higgs measurements, as well as from  $B$  physics, to constrain the parameters  $\rho_{tt}$ ,  $\rho_{bb}$ ,  $\rho_{ct}$ ,  $\rho_{tc}$ , and  $\cos(\beta - \alpha)$  of a general 2HDM that are relevant for observing flavor changing decays of heavy Higgs bosons at the LHC.

### A. Constraints from ATLAS and CMS

Run 1 of LHC at  $\sqrt{s} = 7$  and 8 TeV has provided us with information on the couplings of the Higgs boson  $h^0$ , by measuring the event rates relative to the SM signal strength. Even with our general 2HDM, the light Higgs boson  $h^0$  constitutes a narrow resonance, and the signal strength for a production channel  $X$  and final state  $Y$  can be written as

$$\mu_X(Y) = \frac{\sigma(X) \mathcal{B}(h^0 \rightarrow Y)}{\sigma_{SM}(X) \mathcal{B}(h \rightarrow Y)_{SM}}. \quad (2)$$

ATLAS and CMS often show the signal strength of measurements in two dimensions by grouping gluon fusion and  $tth$  production on one axis (ggF), and vector boson fusion and associated production on the other axis (VBF). These contours can be used to draw constraints on 2HDM's [22]. We follow a simpler approach and consider signal strengths for final states with the largest statistics, namely  $\gamma\gamma$ ,  $ZZ^*$ ,  $WW^*$ , and  $\tau\tau$ , where the dominant production mode is gluon fusion, as well as the signal strength for the  $b\bar{b}$  final state from the associated production  $Vh^0$  with  $V = W$  or  $Z$ . Table I shows the average signal strengths obtained by the experimental groups in Run 1. We combine the ATLAS and CMS results and show both the combined values with their uncertainties in the last column.

To find the allowed regions of 2HDM parameter space compatible with ATLAS and CMS data, we take the discovered Higgs boson as the lightest CP even state ( $h^0$ ) of a general two Higgs doublet model and scan over the following sets of parameters:

$$\begin{aligned} \text{General 2HDM:} \quad & \cos(\beta - \alpha), \rho_{tt}, \rho_{bb}, \rho_{cc}, \rho_{\tau\tau}, \\ \text{Type II 2HDM:} \quad & \cos(\beta - \alpha), \tan\beta. \end{aligned} \quad (3)$$

In SM, the most important contributions to the Higgs total width come from  $b\bar{b}$ ,  $WW^*$ ,  $gg$ ,  $\tau\tau$ ,  $c\bar{c}$  and  $ZZ^*$ . The same channels are expected to contribute in a general 2HDM. In our analysis, we include all the relevant parameters in Eq. (3) that affect the total width, gluon fusion cross section, and the associated Higgs production ( $Vh^0$ ).

We cover a wide range of values for each free parameter, and require that all Yukawa couplings of the mass eigenstates ( $h^0$ ,  $H^0$ ,  $A^0$ ,  $H^\pm$ ) stay perturbative, and that the constraints given in Table I are satisfied. The signal strength for each production and decay channel can be expressed in terms of scale factors which are couplings of the Higgs boson to fermions

Final state	$\mu(\text{ATLAS})$	$\mu(\text{CMS})$	$\mu(\text{comb.})$
$h^0 \rightarrow \gamma\gamma$	$1.17^{+0.27}_{-0.27}$ [23]	$1.14^{+0.26}_{-0.23}$ [24]	$1.16 \pm 0.18$
$h^0 \rightarrow ZZ^* \rightarrow 4\ell$	$1.44^{+0.40}_{-0.33}$ [25]	$0.93^{+0.29}_{-0.25}$ [26]	$1.13 \pm 0.22$
$h^0 \rightarrow WW^* \rightarrow \ell\nu\ell\nu$	$1.09^{+0.23}_{-0.21}$ [27]	$0.72^{+0.20}_{-0.18}$ [28]	$0.89 \pm 0.14$
$h^0 \rightarrow \tau\tau$	$1.43^{+0.43}_{-0.37}$ [29]	$0.78^{+0.27}_{-0.27}$ [30]	$0.99 \pm 0.22$
$h^0 \rightarrow b\bar{b}$	$0.52^{+0.40}_{-0.40}$ [31]	$1.00^{+0.50}_{-0.50}$ [32]	$0.71 \pm 0.31$

TABLE I: Signal strengths for the Higgs boson at the LHC. The last column is our combination. The combined signal strength for  $h^0 \rightarrow WW^* + ZZ^* (VV)$  is  $\mu(VV) = 0.96 \pm 0.12$ .

and gauge bosons normalized to their Standard Model values [33]. These scale factors can then be expressed in terms of the parameters of a specific 2HDM.

Negative results from heavy Higgs searches provide us further insights on the parameter space of an extended Higgs sector. One of the strongest results comes from the search for a heavy Higgs decaying into the  $WW$  and  $ZZ$  final states, excluding a heavy Higgs boson with SM like couplings all the way up to 1 TeV [34]. We use these results to further constraint the parameter space of 2HDM.

In Fig. 1, we present the 68% (95%) confidence level (C.L.) regions in dark (light) color that are compatible with LHC constraints from the light Higgs boson ( $h^0$ ) alone as well as constraints from both the light Higgs boson and the heavy Higgs boson ( $H^0$ ) decaying into  $WW$  and  $ZZ$  [34] for a general 2HDM and a Type-II 2HDM. This figure shows that a large value of  $|\cos(\beta - \alpha)|$  is still a possibility within a general model for  $\rho_{tt} < 1$ . This is due to the lack of a strong constraint on the  $b$ -quark coupling of the Higgs boson. To be consistent with the SM Higgs cross section from gluon fusion, a small value of  $\cos(\beta - \alpha)$  is favored for  $\rho_{tt} \gg 1$  with  $\lambda_{htt} \sim \lambda_{htt}^{SM} = \kappa_{tt}$ . Experimental data from Run 2 with higher energy and higher luminosity will provide much better guidance for parameters such as  $\rho_{tt}$  and  $\cos(\beta - \alpha)$ .

## B. Constraints from $B$ Physics

The FCNH coupling  $\rho_{ct}$  affects the  $H^+tq$  couplings ( $q = d, s, b$ ) through  $(\rho^{U^\dagger V})_{tq} = \rho_{tt}^* V_{tq} + \rho_{ct}^* V_{cq} + \rho_{ut}^* V_{uq}$ . This effect contributes to FCNC processes in down-type quark sector via  $H^+$  and  $t$  loops. For simplicity, let us assume  $\rho_{ut}$  is negligible.

Recasting the 2HDM-II expression [35], we estimate the modifications to the  $B_q\text{-}\bar{B}_q$  ( $q = d, s$ ) mixing amplitude ( $M_{12}^q$ ) from the box diagrams with internal  $H^+/W$  and  $t$  by

$$\frac{M_{12}^q}{[M_{12}^q]_{\text{SM}}} = 1 + \frac{I_{WH}(y^W, y^H, x) + I_{HH}(y^H)}{I_{WW}(y^W)}, \quad (4)$$

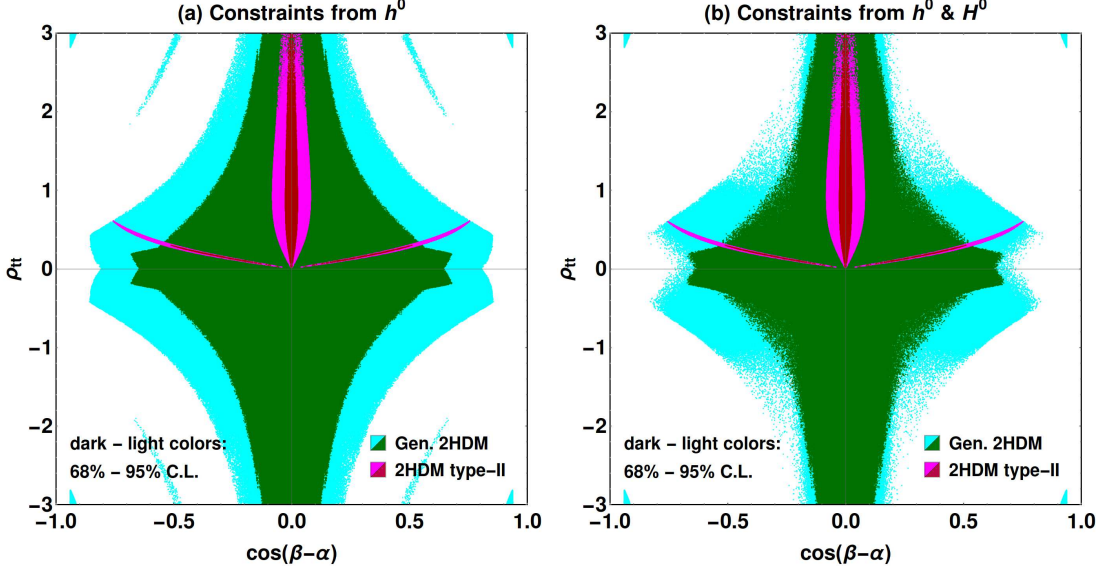


FIG. 1: Favored regions in  $\cos(\beta-\alpha)$ - $\rho_{tt}$  plane at 68% (95%) C.L. of LHC Higgs data in a general 2HDM [green, (light cyan)] and Type II 2HDM [red, (light magenta)], with constraints from (a) light Higgs boson ( $h^0$ ), (b) both light Higgs boson ( $h^0$ ) and heavy Higgs boson ( $H^0$ ).

where  $y^i = m_i^2/m_W^2$  ( $i = W, H^+$ ),  $x = m_{H^+}^2/m_W^2$ , and

$$\begin{aligned}
 I_{WW} &= 1 + \frac{9}{1-y^W} - \frac{6}{(1-y^W)^2} - \frac{6}{y^W} \left( \frac{y^W}{1-y^W} \right)^3 \ln y^W, \\
 I_{WH} &\simeq \left( \frac{\rho_{tt}^*}{\kappa_t} + \frac{V_{cb}\rho_{ct}^*}{V_{tb}\kappa_t} \right) \left( \frac{\rho_{tt}}{\kappa_t} + \frac{V_{cq}\rho_{ct}}{V_{tq}\kappa_t} \right) y^H \\
 &\quad \times \left[ \frac{(2x-8)\ln y^H}{(1-x)(1-y^H)^2} + \frac{6x\ln y^W}{(1-x)(1-y^W)^2} - \frac{8-2y^W}{(1-y^W)(1-y^H)} \right], \\
 I_{HH} &\simeq \left( \frac{\rho_{tt}^*}{\kappa_t} + \frac{V_{cb}\rho_{ct}^*}{V_{tb}\kappa_t} \right)^2 \left( \frac{\rho_{tt}}{\kappa_t} + \frac{V_{cq}\rho_{ct}}{V_{tq}\kappa_t} \right)^2 y^H \left[ \frac{1+y^H}{(1-y^H)^2} + \frac{2y^H\ln y^H}{(1-y^H)^3} \right].
 \end{aligned} \tag{5}$$

We adopt the following intervals from the Summer 2014 results by UFit [36],

$$\begin{aligned}
 C_{B_d} &\in [0.76, 1.43], \quad \phi_{B_d} \in [-8.0^\circ, 4.4^\circ], \\
 C_{B_s} &\in [0.9, 1.23], \quad \phi_{B_s} \in [-3.0^\circ, 4.7^\circ],
 \end{aligned} \tag{6}$$

at 95% probability, where  $C_{B_q} e^{2i\phi_{B_q}} \equiv M_{12}^q/[M_{12}^q]_{\text{SM}}$ .

The constraints from  $B_{d,s}$  mixing data are shown in Fig. 2(a) on the  $(\rho_{tt}, \rho_{ct})$  plane with  $m_{H^+} = 500$  GeV. Shaded regions are excluded by the 95% probability ranges in Eq. (6). The constraint from  $C_{B_s}$  (pink regions) is slightly tighter than the  $C_{B_d}$  exclusion (blue-shaded regions). Combining them with constraint from the  $CP$ -violating phase  $\phi_{B_d}$  (light-green regions), we obtain the upper limit  $|\rho_{tt}| \lesssim 1.5$ , regardless of  $\rho_{ct}$ . The parameter  $\rho_{ct}$  is strongly constrained since its effect in Eq. (5) is enhanced by the CKM factor  $|V_{cq}/V_{tq}| \sim 25$  ( $q = d, s$ ). Once  $\rho_{tt}$  is fixed within this range, we obtain a constraint on  $\rho_{ct}$ . For  $0.5 \lesssim |\rho_{tt}| \lesssim 1.5$ , we

have  $|\rho_{ct}| \lesssim 0.06$ . Furthermore, the sizable phase in  $V_{cd}/V_{td}$  makes  $\rho_{ct}$  sensitive to the  $CP$ -violating phase  $\phi_{B_d}$ , even if  $\rho_{ct}$  is real. For  $m_{H^+} = 300$  (700) GeV, the constraints become:  $|\rho_{tt}| \lesssim 1.2$  (1.8) regardless of  $\rho_{ct}$ , and  $|\rho_{ct}| \lesssim 0.05$  (0.09) for  $0.5 \lesssim |\rho_{tt}| \lesssim 1.2$  (1.8).

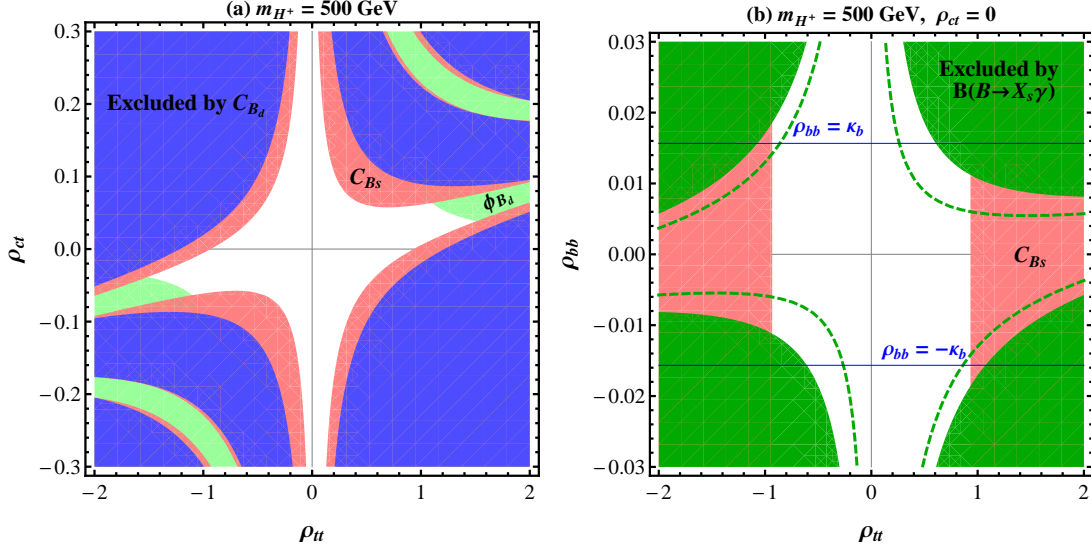


FIG. 2: Allowed regions in (a)  $\rho_{tt}$ - $\rho_{ct}$  plane from  $B_{d,s}$ -mixing, with shaded regions excluded by Eq. (6), i.e. blue (pink) regions by  $C_{B_{d(s)}}$ , light-green regions by  $\phi_{B_d}$ ; (b)  $\rho_{tt}$ - $\rho_{bb}$  plane from  $b \rightarrow s\gamma$  with  $\rho_{ct} = 0$  and  $m_{H^+} = 500$  GeV, with dark-green shaded regions excluded by  $R_{\text{exp}}^{b \rightarrow s\gamma}$  in Eq. (8) at  $2\sigma$ , while pink regions by  $C_{B_s}$ . Blue-solid lines in (b) mark  $|\rho_{bb}| = \kappa_b$  with  $m_b(\mu = m_t)$ .

We now turn to the  $b \rightarrow s\gamma$  constraint. The  $H^+-t$  loop affects this process via the Wilson coefficients  $C_{7,8}$  at leading-order (LO), which are, at the matching scale  $\mu_0$ , given by

$$\delta C_{7,8} \simeq \frac{1}{3} \left( \frac{\rho_{tt}^*}{\kappa_t} + \frac{V_{cb}\rho_{ct}^*}{V_{tb}\kappa_t} \right) \left( \frac{\rho_{tt}}{\kappa_t} + \frac{V_{cs}^*\rho_{ct}}{V_{ts}^*\kappa_t} \right) F_{7,8}^{(1)}(y^H) - \left( \frac{\rho_{tt}}{\kappa_t} + \frac{V_{cs}^*\rho_{ct}}{V_{ts}^*\kappa_t} \right) \frac{\rho_{bb}}{\kappa_b} F_{7,8}^{(2)}(y^H). \quad (7)$$

Here, the operator basis and the definition of  $F_{7,8}^{(1,2)}(y)$  follow Ref. [37]. We follow the procedure in Ref. [38] and calculate first the ratio

$$R_{\text{exp}}^{b \rightarrow s\gamma} = \frac{\mathcal{B}(B \rightarrow X_s \gamma)_{\text{exp}}}{\mathcal{B}(B \rightarrow X_s \gamma)_{\text{SM}}}, \quad (8)$$

with world average of measurements  $\mathcal{B}(B \rightarrow X_s \gamma)_{\text{exp}} = (3.43 \pm 0.21 \pm 0.07) \times 10^{-4}$  [39] and the next-to-next-to LO (NNLO) prediction in SM,  $\mathcal{B}(B \rightarrow X_s \gamma)_{\text{SM}} = (3.15 \pm 0.23) \times 10^{-4}$  [40]. We then require the similar ratio based on our LO calculation, i.e.  $R_{\text{theory}}^{b \rightarrow s\gamma} = \mathcal{B}(B \rightarrow X_s \gamma)_{\text{2HDM}} / \mathcal{B}(B \rightarrow X_s \gamma)_{\text{SM}}$ , to be within the range allowed by  $R_{\text{exp}}^{b \rightarrow s\gamma}$ . Choosing the matching scale and the low-energy scale as  $\mu_0 \sim m_t$  and  $\mu_b \sim m_b/2$ , we reproduce the NNLO results of Ref. [41],  $m_{H^+} \geq 380$  GeV, with 95% C.L. in the Type-II 2HDM<sup>1</sup>.

Fig. 2(b) shows the allowed region in the  $(\rho_{tt}, \rho_{bb})$  plane from  $b \rightarrow s\gamma$  and  $B$  mixing for  $m_{H^+} = 500$  GeV and  $\rho_{ct} = 0$ . The dark-green shaded regions are excluded by the  $2\sigma$

<sup>1</sup> Recent NNLO calculation [42] provides a stronger limit ( $m_{H^+} \geq 480$  GeV) at 95% C.L.



experimental error of  $R_{\text{exp}}^{b \rightarrow s\gamma}$  in Eq. (8), with the theoretical uncertainty linearly added. The constraint on  $\rho_{tt}$  by  $C_{B_s}$  is also shown. For  $\rho_{tt} \sim \kappa_t \sim 1$ ,  $\rho_{bb}$  is constrained to be within  $-0.02 \lesssim \rho_{bb} \lesssim 0.01$ . Note that this touches the region of  $|\rho_{bb}| \sim \kappa_b \sim 0.02$ . We set  $\rho_{ct} = 0$  as it is already strongly constrained by  $B_{d,s}$  mixing. For  $m_{H^+} = 300$  (700) GeV, the  $b \rightarrow s\gamma$  constraint on  $\rho_{bb}$  becomes:  $-0.009$  ( $-0.03$ )  $\lesssim \rho_{bb} \lesssim 0.008$  (0.02) for  $\rho_{tt} \sim 1$ . Typically,  $\mathcal{B}(B \rightarrow X_s \gamma)$  constrains  $\rho_{bb}$  more strongly than  $\rho_{tt}$ , as the effect of  $\rho_{bb}$  is enhanced by the chiral factor  $\kappa_t/\kappa_b = m_t/m_b$  in Eq. (7).

The contribution from charm loop has a mild dependence on  $\rho_{tc}$  through the  $H^+$  couplings,  $(\rho^{U\dagger}V)_{cq} = \rho_{tc}^* V_{tq} + \rho_{cc}^* V_{cq} + \rho_{uc}^* V_{uq}$  ( $q = d, s, b$ ). In general,  $\rho_{tc}$  may be very different from  $\rho_{ct}$ . Since the charm quark in the loop is light and there is no CKM enhancement, the constraint on  $\rho_{tc}$  is expected to be much weaker. The constraint on  $\rho_{tc}$  has been analyzed in Ref. [38]. With  $-\epsilon_{32}^u = \rho_{tc} \sin \beta$ , it is found from  $B_s$  mixing that  $|\epsilon_{32}^u| \leq 1.7$  for  $m_{H^+} = 500$  GeV and  $\tan \beta = 50$ . This constraint implies that  $|\rho_{tc}| \lesssim 1.7$  for  $m_{H^+} = 500$  GeV. We note that a large  $\rho_{tc}$  can enhance  $B \rightarrow D^{(*)} \tau \nu$  rates via the  $H^+$  coupling  $(\rho^{U\dagger}V)_{cb}$  and can explain the  $3.4\sigma$  discrepancy between the SM prediction and BaBar data [43–45]. For real valued  $\rho_{tc}$  and  $\rho_{\tau\tau}$ , the solution space shown in Ref. [38] reads  $\rho_{tc} \sim 0.7 \times (-0.5/\rho_{\tau\tau})(m_{H^+}/500 \text{ GeV})^2$ . Additional flavor constraints can be obtained from  $K - \bar{K}$  mixing ( $\rho_{ct} \lesssim 0.14$ ) [38] and  $D - \bar{D}$  mixing ( $|\rho_{tc}\rho_{tu}^*| \lesssim 0.02$ ) [38] for  $m_H \simeq m_{H^+} = 500$  GeV. The value of  $(\rho_{tu})$  is expected to be very small, thus  $B - \bar{B}$  mixing provides a better limit for  $\rho_{tc}$ .

Combining experimental limits from LHC Higgs data and  $B$  physics, and assuming perturbativity, we consider  $\rho_{tt} < 2$ ,  $\rho_{tc} < 1.5$ , and  $\rho_{ct} < 0.1$ .

### III. SIGNAL AND BACKGROUND

We now discuss the prospects of discovering FCNH interactions at the LHC through  $H^0$  and  $A^0$  decays. The number of free parameters in a general 2HDM is too large for a comprehensive collider study of the FCNH signal, so we make some assumptions that are motivated by experiment. The latest experimental results point to a Higgs sector with the light CP even state behaving like the SM Higgs, indicating that  $\cos(\beta - \alpha)$  should be small. We consider sample cases with  $\cos(\beta - \alpha) = 0.1$  and  $0.2$ , which imply  $\sin(\beta - \alpha) \sim 1$ .

In our case study, we choose the heavier states ( $H^0$ ,  $A^0$  and  $H^\pm$ ) to be degenerate for simplicity, which is also in accordance with the decoupling limit [19], and we set  $\lambda_{6,7} = 0$  in the Higgs potential [9]. We also set  $\tan \beta = 1$  and choose  $m_{12}^2$  such that the scalar potential satisfies stability, tree-level unitarity, and perturbativity up to large masses.

To fix the Yukawa couplings, we assume that  $\rho_{tt} = \kappa_t$  while  $\rho_{bb} = \kappa_b$ . This is in good agreement with both  $B$  physics constraints as well as LHC Run 1 constraints. For the off-diagonal parts that generate the flavor changing signal,  $\rho_{ct}$  is constrained to small values by  $B$  physics but we assume that  $\rho_{tc}$  can have larger values. In the massless limit for charm, the signal cross section is, to a very good approximation, only a function of a single effective coupling  $\tilde{\rho}_{tc} = \frac{1}{\sqrt{2}} \sqrt{\rho_{tc}^2 + \rho_{ct}^2}$ , but also very weakly depends on  $\frac{1}{\sqrt{2}} \sqrt{\rho_{tc}^2 - \rho_{ct}^2}$ . The contribution to the cross section from terms with  $\tilde{\rho}_{tc}$  is at least 98% without cuts and more than 93% with all cuts for  $pp \rightarrow H \rightarrow b c \ell \nu + X$  with  $m_H = 1$  TeV, and it is even more dominating for a lower Higgs mass.

With these experimentally motivated choices, gluon fusion is the dominant production mode for  $H^0$  and  $A^0$  states, and  $t\bar{t}$  becomes the dominant final state at high mass ( $2m_t < m_\phi \lesssim 2$  TeV). We display in Fig. 3 the branching fractions for (a) the heavier scalar  $H^0$ , and (b) the pseudoscalar  $A^0$ , as functions of Higgs mass with  $\cos(\beta - \alpha) = 0.1$  and  $\tilde{\rho}_{tc} =$

0.24. The computer code 2HDMC [46] is employed to scan over  $|m_{12}| \leq 2$  TeV and  $0.1 \leq \tan \beta \leq 50$  with sets of parameters that satisfy potential stability, tree-level unitarity, and perturbativity. This gives rise to the “bands” in Fig. 3(a). We also display the branching fraction  $\mathcal{B}(H^0 \rightarrow tc)$  for the aforementioned choice of  $\tan \beta$  and  $m_{12}^2$  in our LHC case study with a dashed curve in Fig. 3(a). We note that with large branching fraction in most of the parameter space,  $H^0 \rightarrow h^0 h^0$  might offer great promise to discover Higgs pairs at the LHC.

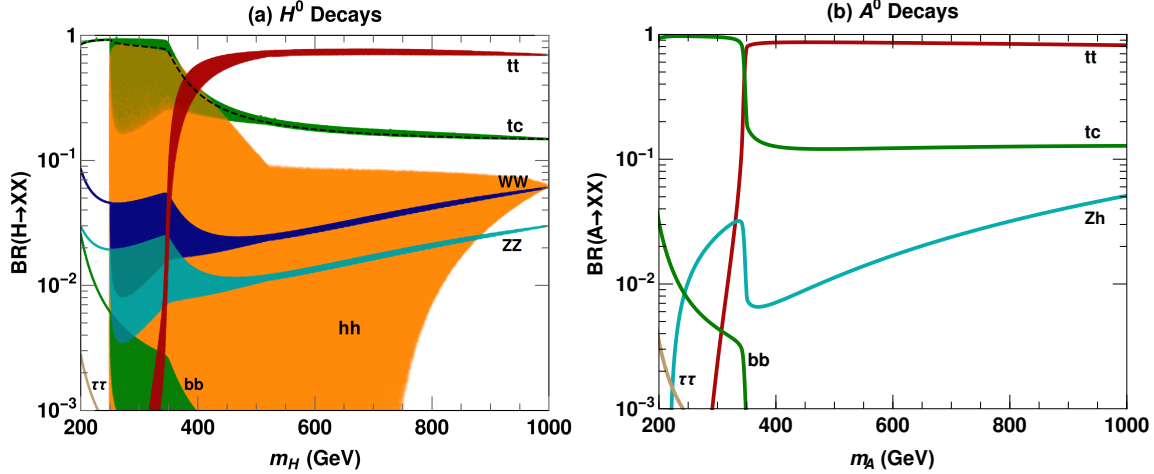


FIG. 3: Branching fraction of (a) heavier Higgs scalar  $H^0$  and (b) Higgs pseudoscalar  $A^0$  versus  $m_\phi$ , with  $\cos(\beta - \alpha) = 0.1$ ,  $\tilde{\rho}_{tc} = 0.24$ , and  $\rho_{ii} = \kappa_i$  for diagonal couplings. We show the allowed regions when  $\tan \beta$  and  $m_{12}^2$  are varied. Branching fraction  $\mathcal{B}(H^0 \rightarrow tc)$  for the LHC case study is shown as a dashed curve.

### A. Higgs Signal

Our signal is the production of a heavy Higgs boson from gluon fusion, with subsequent flavor changing decays into a charm quark and a top quark, and the top decays semileptonically. More explicitly, we consider  $gg \rightarrow \phi^0 \rightarrow t\bar{c} + \bar{t}c$  ( $\phi^0 = H^0$  or  $A^0$ ), followed by  $t\bar{c} \rightarrow b\ell\nu\bar{c}$  with  $\ell = e$  or  $\mu$ . Unless explicitly specified,  $q$  generally denotes a quark ( $q$ ) or an anti-quark ( $\bar{q}$ ) and  $\ell$  represents a lepton ( $\ell^-$ ) or anti-lepton ( $\ell^+$ ). We calculate the matrix elements analytically, and compute the signal cross section with the parton distribution functions of MSTW2008 [47]. The factorization and renormalization scales are chosen to be  $\mu_{F,R} = m_\phi$ . In addition, to estimate the NLO cross section for  $pp \rightarrow \phi^0 \rightarrow t\bar{c} + \bar{t}c \rightarrow b\ell\nu c + X$ , we use the computer code HIGLU [48] to calculate  $\sigma(pp \rightarrow \phi^0 + X)$  ( $\phi^0 = H^0, A^0$ ), including both top and bottom quark loops to find a  $K$ -factor.

### B. Standard Model Background

The dominant physics background to the final state of  $bj\ell\nu$  comes from  $Wjj + Wb\bar{b}$ , as well as  $s$ - and  $t$ -channel single top ( $tb + tj$ ). Another important background is  $t\bar{t}$  production where either one of the two leptons is missed for both top quarks decaying semileptonically, or two of the four jets are missed when only one of top quarks decays semileptonically.



We employ the programs MadGraph [49, 50] and HELAS [51] to evaluate the exact matrix elements for the background processes. The factorization and the renormalization scales are chosen to be  $\mu_{R,F} = m_W$  for  $Wjj$  and  $Wb\bar{b}$ ,  $\mu_{R,F} = m_t$  for  $s$ - and  $t$ -channel single top, and  $\mu_{R,F} = \sqrt{s}$  for  $t\bar{t}$ . We use MCFM [52] to calculate the NLO  $K$ -factors for our background processes.

### C. Mass Reconstruction

Let us present our strategy for full reconstruction of each event with the help of intermediate on-shell particles. For each event, we require one  $b$  jet and one non- $b$  jet, identified through  $b$ -tagging. In addition, we require a single isolated lepton and missing transverse energy from the neutrino in the semileptonic decay of the top quark in our FCNH signal. For lepton momentum  $p$  and neutrino momentum  $k$ , the invariant mass constraint for an on-shell  $W$ ,  $(k + p)^2 = m_W^2$ , can be solved for the longitudinal component of the neutrino momentum ( $k_z$ ), which is the only unknown in the event. We obtain two solutions

$$k_z^\pm = \frac{p_z(2\mathbf{k}_T \cdot \mathbf{p}_T + m_W^2 - m_\ell^2) \pm E_\ell \Delta}{2(m_\ell^2 + p_T^2)}, \Delta^2 = (2\mathbf{k}_T \cdot \mathbf{p}_T + m_W^2 - m_\ell^2)^2 - 4k_T^2(m_\ell^2 + p_T^2). \quad (9)$$

If  $\Delta^2 < 0$  hence  $k_z^\pm$  complex, the event is vetoed. For  $\Delta^2 > 0$  with  $k_z^\pm$  real, we choose the solution that minimizes the reconstructed top mass  $|M_{b\ell\nu} - m_t|$  or  $|(p_b + p + k)^2 - m_t^2|$ .

Systematics can be the limiting factor for new physics searches at high luminosities. Precise determination of the background needs to include systematics in experiments. Since our signal is a sharp peak over a smoothly falling background, the precise knowledge of background cross section at percent level is not required for a  $5\sigma$  discovery. An uncertainty of 30% in the background estimation might shift the limit on  $g_{Htc}$  by 10% without affecting our results.

### D. Realistic Acceptance Cuts

To study the discovery potential, we employ three sets of realistic cuts and tagging efficiencies. For low luminosity (LL): (a) LHC Run 1 ( $\sqrt{s} = 8$  TeV) with  $L = 25 \text{ fb}^{-1}$  [53]; and (b) full CM energy ( $\sqrt{s} = 13$  or 14 TeV) with  $L = 30 \text{ fb}^{-1}$ . For high luminosity (HL): (c) full CM energy ( $\sqrt{s} = 14$  TeV) with  $L = 300 \text{ fb}^{-1}$  or  $3000 \text{ fb}^{-1}$  [54, 55].

We require that in every event there should be (a) exactly 2 jets that have  $p_T > 20$  GeV (30 GeV for HL) and  $|\eta| < 2.5$ , and one of them must be tagged as a  $b$ -jet; (b) exactly one isolated lepton that has  $p_T > 20$  GeV and  $|\eta| < 2.5$ ; (c) at least 20 GeV (40 GeV for HL) of missing transverse energy ( $\cancel{E}_T$ ). After reconstructing the longitudinal component of the neutrino momentum, we further require that (d) the reconstructed invariant mass of the top satisfies  $|m_{b\ell\nu} - m_t| < 0.2 m_t$ ; (e) the reconstructed invariant mass of the Higgs boson satisfies  $|m_{b\ell\nu c} - m_\phi| < 0.2 m_\phi$ .

We consider a further powerful acceptance cut on non- $b$ -tagged jet momentum. In the Higgs boson decay frame, the charm quark momentum from  $H^0, A^0 \rightarrow tc$  is approximately given by

$$p_c \approx \frac{m_\phi}{2} \left[ 1 - \frac{m_t^2}{m_\phi^2} \right]. \quad (10)$$

Since the Higgs boson from gluon fusion has little transverse momentum, the  $p_T(c)$  distribution has both a kinematic cut-off and a peak at the above  $p_c$  value. We require that the transverse momentum of the non- $b$ -tagged jet satisfies  $0.85 p_c < p_T(c) < 1.10 p_c$ .

To simulate detector effects based on ATLAS [54] and CMS [55] specifications, we apply Gaussian smearing of momenta:

$$\frac{\Delta E}{E} = \frac{0.60}{\sqrt{E(\text{GeV})}} \oplus 0.03 \quad (\text{jets}), \quad \text{and} \quad \frac{\Delta E}{E} = \frac{0.25}{\sqrt{E(\text{GeV})}} \oplus 0.01 \quad (\text{leptons}), \quad (11)$$

with individual terms added in quadrature ( $\oplus$ ). In LHC Run 1 at  $\sqrt{s} = 8$  TeV, the  $b$ -tagging efficiency ( $\epsilon_b$ ) is taken to be 50%, the probability that a  $c$ -jet is mistagged as a  $b$ -jet ( $\epsilon_c$ ) is 14% and the probability that any other jet is mistagged as a  $b$ -jet ( $\epsilon_j$ ) is taken to be 1%. At the full CM energy ( $\sqrt{s} = 13$  or 14 TeV) with  $L = 30 \text{ fb}^{-1}$ , we follow the tagging and mistag efficiencies in the ATLAS Technical Design Report [54]:  $\epsilon_b = 60\%$ ,  $\epsilon_c = 14\%$  and  $\epsilon_j = 1\%$ . For the full CM energy ( $\sqrt{s} = 13$  or 14 TeV) with HL of  $300 \text{ fb}^{-1}$  or  $3000 \text{ fb}^{-1}$ , the tagging and mistag efficiencies are taken to be  $\epsilon_b = 50\%$ ,  $\epsilon_c = 14\%$  and  $\epsilon_j = 1\%$ .

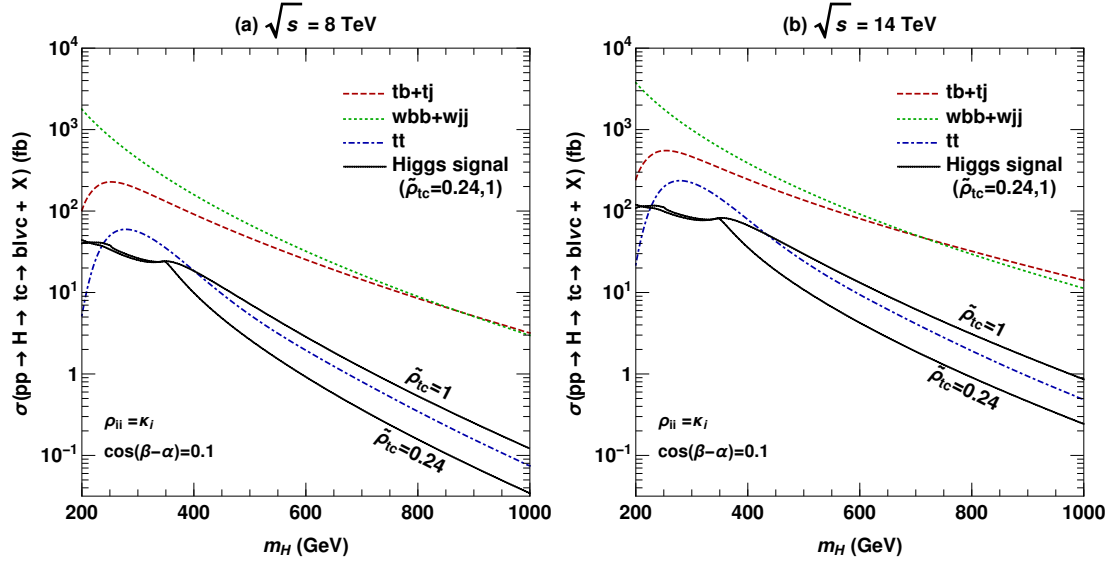


FIG. 4: The cross section of the heavier Higgs scalar  $H^0$  (solid)  $\sigma(pp \rightarrow H^0 \rightarrow t\bar{c} + \bar{t}c \rightarrow bj\ell + \cancel{E}_T + X)$  at the LHC versus  $m_H$  for (a)  $\sqrt{s} = 8$  TeV and (b)  $\sqrt{s} = 14$  TeV, with  $\tilde{\rho}_{tc} = 0.24, 1$  and  $\cos(\beta - \alpha) = 0.1$ . Also shown are the background cross sections (dashed) from single top ( $tb$  and  $tj$ ),  $W$ +jets ( $Wjj$  and  $Wbb$ ) and  $t\bar{t}$  with  $K$ -factors, acceptance cuts, and tagging efficiencies.

#### IV. DISCOVERY POTENTIAL

We present the signal and background cross sections at the LHC for  $\sqrt{s} = 8$  TeV and 14 TeV in Fig. 4. All tagging efficiencies and  $K$ -factors discussed above are included. We observe that the largest contributions to the SM background come from single-top and  $W$ +jets processes, which is to be expected, since they can both produce very similar kinematics to our signal process. In contrast, the  $t\bar{t}$  background is substantially lower because of the requirement on the number of jets and leptons passing our cuts.

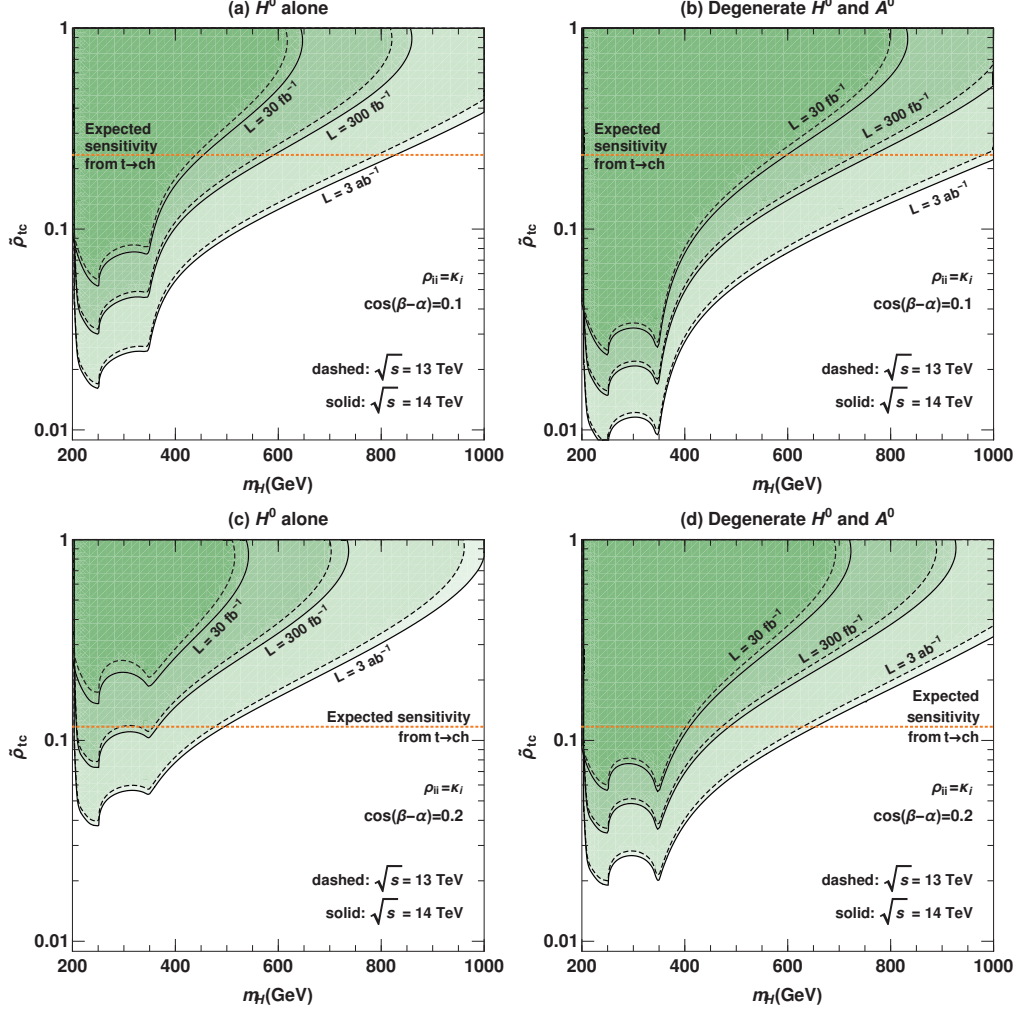


FIG. 5: Discovery reach at  $5\sigma$  in the  $m_\phi$ - $\rho_{tc}$  plane for the  $pp \rightarrow \phi^0 \rightarrow t\bar{c} + \bar{t}c \rightarrow bj\ell + \cancel{E} + X$  signal at the LHC with  $\sqrt{s} = 13$  (14) TeV for dashed (solid) contours. (a) is for the heavier Higgs scalar ( $H^0$ ) and (b) for the combined  $H^0$  and  $A^0$  assuming degeneracy, both for  $\cos(\beta - \alpha) = 0.1$ . (c) and (d) are analogous, but for  $\cos(\beta - \alpha) = 0.2$ . The discovery region is the parameter space above the contours. Also shown is the future ATLAS sensitivity at 95 % confidence level for  $t \rightarrow ch^0 \rightarrow c\gamma\gamma$ .

To estimate the discovery potential, we obtain the lower limit on  $\sigma_S$  by requiring that the 99.4%-confidence-level (CL) upper limit on the background is smaller than the 99.4%-CL lower limit on the signal plus background [56] with statistical fluctuations. This leads to the condition,

$$\sigma_S \geq \frac{N}{L} \left[ N + 2\sqrt{L\sigma_B} \right], \quad (12)$$

where  $\sigma_{S(B)}$  is the signal (background) cross section and  $L$  the integrated luminosity. Choosing the parameter  $N = 2.5$  corresponds to  $5\sigma$  significance. For a large number of events ( $L\sigma_B \gg 1$ ), this requirement is equivalent to the statistical significance

$$N_{SS} = \frac{N_S}{\sqrt{N_B}} = \frac{L\sigma_S}{\sqrt{L\sigma_B}} \geq 5,$$

where  $N_{S(B)}$  is the number of signal (background) events.

We show in Fig. 5 the discovery reach in the  $m_\phi\text{--}\tilde{\rho}_{tc}$  plane for the FCNH signal  $pp \rightarrow \phi^0 \rightarrow t\bar{c} + \bar{t}c \rightarrow bj\ell + \cancel{E}$  at the LHC with  $\sqrt{s} = 13$  (14) TeV, for dashed (solid) contours and for  $\cos(\beta - \alpha) = 0.1$  and 0.2. Fig. 5(a,c) are for the heavier scalar  $H^0$  alone, whereas Fig. 5(b,d) are for the degenerate case, for which the scalar  $H^0$  and pseudoscalar  $A^0$  signals are added together. The FCNH decay of the heavy Higgs will be observable for  $\cos(\beta - \alpha) = 0.1$  and  $\tilde{\rho}_{tc} = 0.1$  up to  $m_H \gtrsim 800$  GeV with  $3000 \text{ fb}^{-1}$  data. A larger value of  $\rho_{tc}$  will enhance the cross section, hence statistical significance, of this FCNH signal.

## V. CONCLUSION

In a general two Higgs doublet model, there could be flavor changing neutral Higgs interactions with fermions. Strong limits exist for these FCNH interactions, except those involving the third generation quarks. It is of great interest to study the relation between the most massive elementary particle (the top quark) and the Higgs bosons. The LHC has discovered a Higgs boson lighter than the top, which makes the rare decay  $t \rightarrow ch^0$  kinematically possible. In a general 2HDM, the decay width of  $t \rightarrow ch^0$  is proportional to  $\cos(\beta - \alpha)$ , while that of  $H^0 \rightarrow t\bar{c}$  is proportional to  $\sin(\beta - \alpha)$ . Therefore, they are complementary to each other in the search for new physics beyond the Standard Model.

We investigated the prospects for discovering  $H^0, A^0 \rightarrow t\bar{c}$  at the LHC, where the heavy scalar  $H^0$  and pseudoscalar  $A^0$  are produced via gluon fusion, which are facilitated by the extra  $tt$  couplings. The primary physics background comes from  $Wjj$ ,  $tj$ ,  $Wbb$ ,  $tb$ , and  $t\bar{t}$ . Both signal and background processes are studied with realistic acceptance cuts as well as tagging and mistag efficiencies. Promising results have been found for the LHC with a center of mass energy of 13 TeV and 14 TeV. The FCNH decay of the heavy Higgs will be observable for  $\cos(\beta - \alpha) = 0.1$  and  $\tilde{\rho}_{tc} = 0.1$  up to  $M_H = 800$  GeV with  $3000 \text{ fb}^{-1}$  of integrated luminosity. This result is robust against a small  $\cos(\beta - \alpha)$ , independent of the  $t \rightarrow ch^0$  search, which becomes diminished. If c-tagging efficiency can be improved [57], the discovery potential of this FCNH signal will be greatly enhanced.

If  $\tilde{\rho}_{tc} \gtrsim 0.5$ ,  $\mathcal{B}(H^0 \rightarrow tc)$  can become comparable to  $\mathcal{B}(H^0 \rightarrow t\bar{t})$  or surpass it. Recently, it was suggested that next-to-leading order QCD and electroweak corrections might swamp the signal of Higgs decays into top quark pairs [58]. A recent analysis shows that  $H^0 \rightarrow t\bar{t}$  with SM couplings can be very difficult to observe at the LHC [59]. In that case the FCNH decay of  $H^0, A^0 \rightarrow t\bar{c} + \bar{t}c$  might offer a promising opportunity to observe the heavier Higgs bosons.

We have not emphasized the  $\tau$  lepton sector. Recently, the CMS Collaboration reported unexpected  $\tau\mu$  events [60] that might be explained by neutral Higgs boson decay [61]. If this can be confirmed by the ATLAS collaboration in the near future, or at LHC Run 2, it will be exciting new physics for FCNH interactions, and  $H^0, A^0 \rightarrow \tau^\pm \mu^\mp$ , unsuppressed by decoupling (i.e. small  $\cos(\beta - \alpha)$ ), could help discover the exotic scalars.

## Acknowledgments

CK thanks the Academia Sinica, National Taiwan University, and National Center for Theoretical Sciences for excellent hospitality. BA thanks Kyu Jung Bae for discussions. The computing for this project was performed at the OU Supercomputing Center for Education

& Research (OSCEr) at the University of Oklahoma (OU). This research was supported in part by the U.S. Department of Energy under Grant No. DE-FG02-13ER41979 (CK, BA, and BM); the Academic Summit grant MOST 103-2745-M-002-001-ASP, as well as grant NTU-EPR-103R8915 (WSH); and grant NSC 102-2112-M-033-007-MY3 (MK).

- 
- [1] G. Aad *et al.* [ATLAS Collaboration], Phys. Lett. B **716** (2012) 1.
  - [2] S. Chatrchyan *et al.* [CMS Collaboration], Phys. Lett. B **716** (2012) 30.
  - [3] A. K. Das and C. Kao, Phys. Lett. B **372**, 106 (1996).
  - [4] G. Eilam, J. L. Hewett and A. Soni, Phys. Rev. D **44**, 1473 (1991); [Erratum-ibid. D **59**, 039901 (1999)].
  - [5] B. Mele, S. Petrarca and A. Soddu, Phys. Lett. B **435**, 401 (1998).
  - [6] J. A. Aguilar-Saavedra, Acta Phys. Polon. B **35**, 2695 (2004).
  - [7] W.-S. Hou, Phys. Lett. B **296**, 179 (1992).
  - [8] S. L. Glashow and S. Weinberg, Phys. Rev. D **15**, 1958 (1977).
  - [9] J. F. Gunion, H. E. Haber, G. L. Kane and S. Dawson, Front. Phys. **80**, 1 (2000); *The Higgs Hunter's Guide* (Addison-Wesley, Redwood City, CA, 1990).
  - [10] V. D. Barger, J. L. Hewett and R. J. N. Phillips, Phys. Rev. D **41** (1990) 3421.
  - [11] S. Davidson and H. E. Haber, Phys. Rev. D **72**, 035004 (2005) [Phys. Rev. D **72**, 099902 (2005)].
  - [12] F. Mahmoudi and O. Stal, Phys. Rev. D **81** (2010) 035016.
  - [13] J. A. Aguilar-Saavedra and G. C. Branco, Phys. Lett. B **495**, 347 (2000).
  - [14] C. Kao, H.-Y. Cheng, W.-S. Hou and J. Sayre, Phys. Lett. B **716** (2012) 225.
  - [15] K.-F. Chen, W.-S. Hou, C. Kao and M. Kohda, Phys. Lett. B **725** (2013) 378.
  - [16] D. Atwood, S. K. Gupta and A. Soni, JHEP **1410** (2014) 57.
  - [17] CMS Collaboration, CMS-PAS-HIG-13-034 (2014).
  - [18] ATLAS Collaboration, ATL-PHYS-PUB-2013-012 (2013).
  - [19] J. F. Gunion and H. E. Haber, Phys. Rev. D **67** (2003) 075019.
  - [20] N. Craig, J. Galloway and S. Thomas, arXiv:1305.2424 [hep-ph].
  - [21] M. Carena, I. Low, N. R. Shah and C. E. M. Wagner, JHEP **1404** (2014) 015.
  - [22] G. Belanger, B. Dumont, U. Ellwanger, J. F. Gunion and S. Kraml, Phys. Rev. D **88**, 075008 (2013).
  - [23] G. Aad *et al.* [ATLAS Collaboration], Phys. Rev. D **90**, 112015 (2014).
  - [24] V. Khachatryan *et al.* [CMS Collaboration], Eur. Phys. J. C **74**, 3076 (2014).
  - [25] G. Aad *et al.* [ATLAS Collaboration], Phys. Rev. D **91**, 012006 (2015).
  - [26] S. Chatrchyan *et al.* [CMS Collaboration], Phys. Rev. D **89**, 092007 (2014).
  - [27] G. Aad *et al.* [ATLAS Collaboration], arXiv:1412.2641 [hep-ex].
  - [28] S. Chatrchyan *et al.* [CMS Collaboration], JHEP **1401**, 096 (2014).
  - [29] G. Aad *et al.* [ATLAS Collaboration], JHEP **1504**, 117 (2015).
  - [30] S. Chatrchyan *et al.* [CMS Collaboration], JHEP **1405**, 104 (2014).
  - [31] G. Aad *et al.* [ATLAS Collaboration], JHEP **1501**, 069 (2015).
  - [32] S. Chatrchyan *et al.* [CMS Collaboration], Phys. Rev. D **89**, 012003 (2014).
  - [33] A. David *et al.* [LHC Higgs Cross Section Working Group], arXiv:1209.0040 [hep-ph]; and references therein.
  - [34] V. Khachatryan *et al.* [CMS Collaboration], arXiv:1504.00936 [hep-ex].

- [35] C.Q. Geng and J.N. Ng, Phys. Rev. D **38**, 2857 (1988) [Erratum-ibid. D **41**, 1715 (1990)].
- [36] M. Bona *et al.* [UTfit Collaboration], Phys. Rev. Lett. **97**, 151803 (2006); JHEP **0803**, 049 (2008); see <http://www.utfit.org/> for updates.
- [37] M. Ciuchini, G. Degrossi, P. Gambino and G.F. Giudice, Nucl. Phys. B **527**, 21 (1998).
- [38] A. Crivellin, A. Kokulu and C. Greub, Phys. Rev. D **87**, 094031 (2013).
- [39] Y. Amhis *et al.* [Heavy Flavor Averaging Group (HFAG) Collaboration], arXiv:1412.7515 [hep-ex]; see <http://www.slac.stanford.edu/xorg/hfag> for updates.
- [40] M. Misiak *et al.*, Phys. Rev. Lett. **98**, 022002 (2007).
- [41] T. Hermann, M. Misiak and M. Steinhauser, JHEP **1211**, 036 (2012).
- [42] M. Misiak *et al.*, arXiv:1503.01789 [hep-ph].
- [43] S. Fajfer, J.F. Kamenik, I. Nisandzic and J. Zupan, Phys. Rev. Lett. **109**, 161801 (2012).
- [44] A. Crivellin, C. Greub and A. Kokulu, Phys. Rev. D **86**, 054014 (2012).
- [45] J.P. Lees *et al.* [BaBar Collaboration], Phys. Rev. Lett. **109**, 101802 (2012).
- [46] D. Eriksson, J. Rathsmann and O. Stal, Comput. Phys. Commun. **181** (2010) 189.
- [47] A. D. Martin, W. J. Stirling, R. S. Thorne and G. Watt, Eur. Phys. J. C **63**, 189 (2009).
- [48] M. Spira, hep-ph/9510347.
- [49] T. Stelzer and W. F. Long, Comput. Phys. Commun. **81**, 357 (1994).
- [50] J. Alwall *et al.*, JHEP **0709**, 028 (2007).
- [51] H. Murayama, I. Watanabe and K. Hagiwara, KEK-91-11.
- [52] J. M. Campbell and R. K. Ellis, Nucl. Phys. Proc. Suppl. **205-206**, 10 (2010).
- [53] R. J. Steinhausen [for The LHC Team], talk presented at the 36th International Conference on High Energy Physics (ICHEP 2012), Melbourne, Australia, 4–11 July 2012.
- [54] G. Aad *et al.* [ATLAS Collaboration], arXiv:0901.0512 [hep-ex].
- [55] G. L. Bayatian *et al.* [CMS Collaboration], J. Phys. G **34**, 995 (2007).
- [56] H. Baer, M. Bisset, C. Kao and X. Tata, Phys. Rev. D **46**, 1067 (1992).
- [57] ATLAS Collaboration, ATLAS-CONF-2014-046.
- [58] S. Moretti and D. A. Ross, Phys. Lett. B **712** (2012) 245.
- [59] N. Craig, F. D’Eramo, P. Draper, S. Thomas and H. Zhang, JHEP **1506**, 137 (2015) [arXiv:1504.04630 [hep-ph]].
- [60] V. Khachatryan *et al.* [CMS Collaboration], arXiv:1502.07400 [hep-ex].
- [61] R. Harnik, J. Kopp and J. Zupan, JHEP **1303**, 026 (2013).